Adversarial Network in the search for SUSY in events with one lepton and multiple jets in proton-proton collisions

Farouk Mokhtar, University of Science and Technology at Zewail City, Egypt

Supervisors: Ashraf Mohamed, Dirk Kruecker, Isabell Melzer-Pellmann

November 23, 2019

Abstract

In the inclusive single-lepton search published by CMS [ref. 1] for 36.5 $fb^{-}1$ of 13 TeV proton-proton collisions data, a Data-Driven Background Estimation was performed. This search may be improved by the use of machine learning techniques, and to be able to perform similar Data-Driven Background Estimation, the classifier output have to be uncorrelated to one of the event parameters with good signal-to-background separation. To achieve such classification an Adversarial Network was constructed, studied and tested on the same simulation data which was used in the SUSY search by CMS [ref. 1].

Contents

1 Introduction

Although the Standard Model (SM) has demonstrated huge successes in providing experimental predictions, it leaves some phenomena unexplained and falls short of being a complete theory of fundamental interactions. The Hierarchy Problem and Dark Matter are two of the many phenomena that the SM fails to explain. On the other hand, Supersymmetry (SUSY), as an extension to the SM, is a good candidate to solve these two (and other) yet unexplained phenomena. SUSY is a principle that proposes a relationship between two basic classes of elementary particles: bosons, which have an integer-valued spin, and fermions, which have a half-integer spin. In SUSY, each fermion has a supersymmetric boson counterpart (and vice versa). Some of the hypothetical particles, introduced by SUSY, contribute to the correction of the higgs mass and provide solution to the Hierarchy Problem. Also, the SUSY hypothetical LSP is a good candidate for Dark Matter. Hence, the search for SUSY is ongoing, meanwhile, the search relies on the discrimination of the signal from the background SM processes.

Since machine learning techniques provide better signal-to-background classification than cut-based analysis, it is worth to investigate the implementation of Deep Neural Network (DNN) classifiers in the search for SUSY. This work is dedicated to the use of a Neural Network called: Adversarial Network, in the search for SUSY in events with one lepton and multiple jets in proton-proton collisions. The work aims to use Data-Driven Background Estimation (ABCD) method to extrapolate and predict the background in the signal region. To do so, two uncorrelated variables in the analysis are needed, and hence; an Adversarial Network, which decorrelates one of the physics variables from the network's output, is developed.

In section 2, some analysis techniques are presented, and sections 3 and 4 are dedicated to describing the physics problem and presenting the analysis respectively.

2 Analysis Techniques

2.1 Neural Networks

Neural Networks are widely used to deal with regression and classification problems. In physics data analysis, they offer great utility for signal-to-background classification and are conventionally called classifiers. In general, there are three types of machine learning: supervised, semi-supervised and unsupervised. This work focuses on supervised learning, in which after each classification iteration, the network is provided with feedback for comparison and improvement.

The architecture of a Neural Network is identified by:

- The number of hidden layers and nodes which indicates the depth of the network. A network with two or more hidden layers is generally considered deep.

- The activation function which indicates how the output per node is produced from the input.
- The Loss function which translates the output of the network into a scalar, called the loss, to be minimized through training. The value of the loss represents how far is the predicted result from the true values.
- The Optimizer and Learning Rate which control the learning procedure.

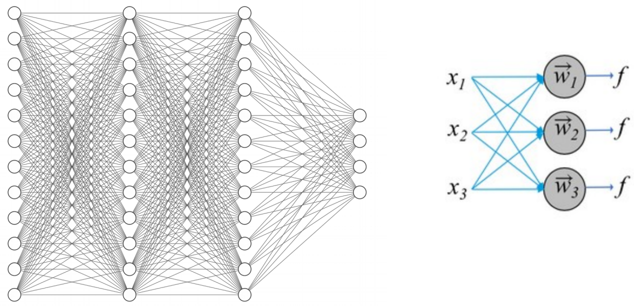

(a) (b)

Figure 1: (a) A typical representation of a Neural Network. (b) A closer look as to how the output is produced per node as explained in the text.

Figure 1b gives a representation as to how the output is produced per node. All inputs x_k are fed to each neuron in the layer. A weighted sum of the inputs and the bias term per neuron are fed to the activation function f to produce the output as follows:

$$f(\sum_{k=1}^{n} w_k x_k + b)$$

The goal of the training is the adjustment of all the weight parameters w_k and bias terms b of the network until the loss stabilizes onto a global minimum.

2.2 Adversarial Networks

Adversarial Networks were first introduced in 2014 [2], and later developped and used for the first time in physics in LHC analysis [3]. An Adversarial Network consists of two Neural Networks: a classifier and an adversary. The classifier is given input data X, with the task of separating signal from background events, while the adversary tries to ensure that the classifier output is independent of one of the features: $Z \in X$ or $Z(X)$. This comes at the expense of classification efficiency. Due to the brought about loss in efficiency, the adversary is said to have confused the classifier.

The two networks are coupled in a way that the training is done simultaneously, and the combined loss to be minimized is given by:

$$loss = loss_{clf} - \lambda \cdot loss_{adv}$$

The parameter λ is accordingly added to the network hyper-parameter space to be optimized. It defines the activity of the adversary. A greater value of λ indicates high adversary activity, which results in high confusion. An optimal value of λ allows for the decorrelation at the expense of little classification efficiency loss.

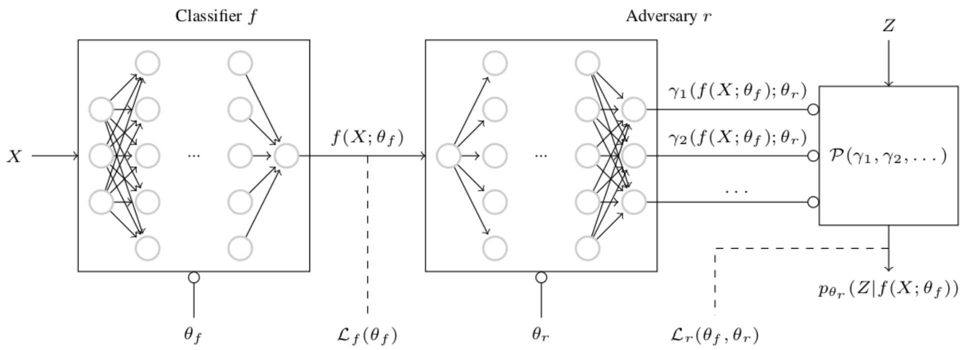

Figure 2: A general representation of an Adversarial Network (as presented in [3]).

2.3 Data-Driven Background Estimation

If two variables var_1 and var_2 are uncorrelated, then in Figure 3, background in signal region can be predicted using the following formula:

$$N_D = N_C \cdot \frac{N_A}{N_B}$$

where N refers to the number of background events and the subscript refers to the part of the graph where the event resides.

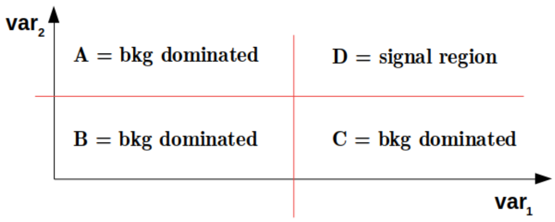

Figure 3: A diagram defining the ABCD regions for two variables when using Data-Driven Background Estimation.

3 Physics Problem

In this work, events with a single lepton and multiple jets resulting from proton-proton collisions are studied. A simplified model of the signal process begins with a gluino pair production, each gluino then decays into top-anti-top pair ($t\bar{t}$) and LSP ($\tilde{\chi}_0$), also called neutralino. Each top quark then decays into a W-boson and b-jets. The studied signal corresponds to one W-boson leptonic decay and three W-boson hadronic decays. In this process, both the LSP and the neutrino result in the missing transverse energy (MET), unlike the background standard model processes where only the neutrino results in all the MET. Feynman Diagrams representing the signal and two main backgrounds are shown in Figure 4a and Figure 4b respectively.

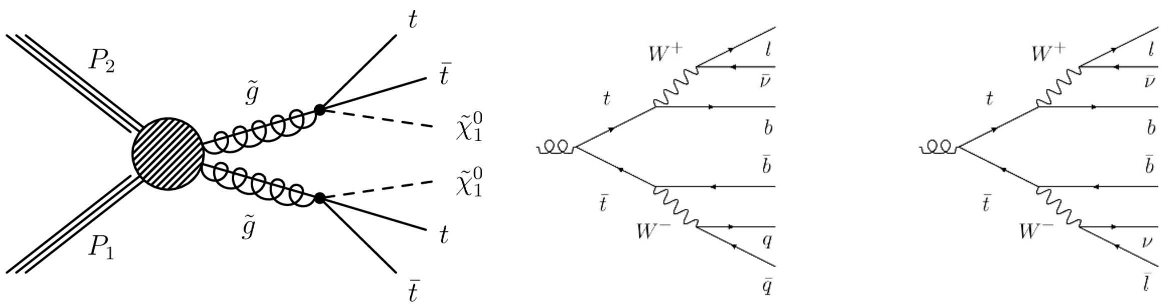

(a) (b)

Figure 4: (a) Feynman diagram describing the signal process. (b) Feynman diagrams describing the two main background.

One of the main search variables in the analysis is an angle between the reconstructed W-boson and lepton, $\Delta\varphi$, since this angle has a discrimination power between signal and background. A representation of $\Delta\varphi$, for both models, is shown in Figure 5.

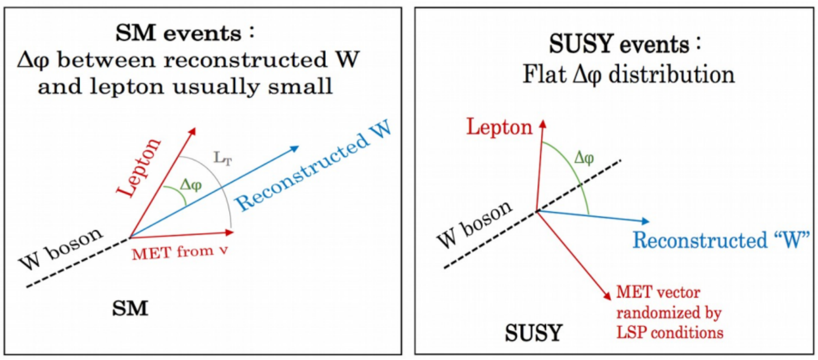

Figure 5: Two pictures representing $\Delta\varphi$ (in green) for the SM and SUSY respectively. As can be seen, it is the angle between the lepton and the reconstructed boson.

In 2016, a search for SUSY in events with a single electron or muon in proton-proton collisions at a center-of-mass energy of 13 TeV, was performed [1]. The data were recorded by the CMS experiment at the LHC and the observed event yields in data were found consistent with the expected backgrounds from standard model processes. The distribution of data and Monte Carlo events as a function of $\Delta\varphi$, are shown in Figure 6, and it is clear that the main backgrounds peak at small values of $\Delta\varphi$. Therefore, the signal region was defined for $\Delta\varphi > 1$.

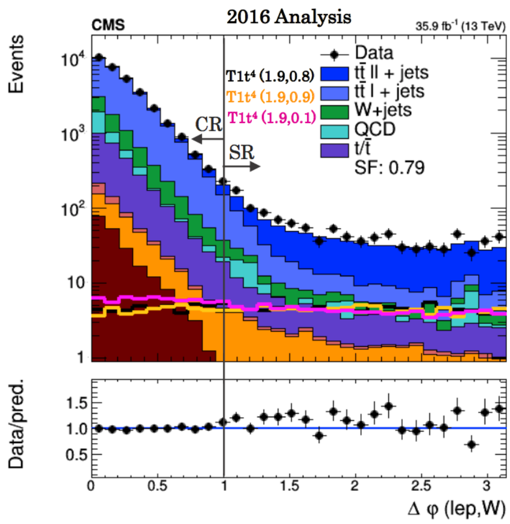

Figure 6: The distribution of data and Monte Carlo events as a function of $\Delta\varphi$. The three main backgrounds are: $t\bar{t} \rightarrow ll$ (represented in dark blue), $t\bar{t} \rightarrow l$ (represented in light blue) and Wjets (represented in dark green). Note how background events are concentrated near small $\Delta\varphi$ indicating that this angle has a discrimination power between signal and background.

3.1 Motivation

Since machine learning techniques provide better signal-to-background classification than cut-based analysis, it is worth to investigate how the analysis could be improved using a Deep Neural Network (DNN) classifier. To predict background in the signal region with the ABCD method, the classifier output should be uncorrelated to $\Delta\varphi$. To obtain such classifier, an Adversarial Network, as described in section 2.2, was developed.

4 Analysis

The search for the most efficient Adversarial Network amounts to finding the optimal value of λ which provides the decorrelation at the lowest classification efficiency loss. The optimal value of λ is the one which gives the Ratio: $\frac{N_A/N_B}{N_D/N_C} = 1$ (see Figure 3).

4.1 Results for the classifier

In physics analysis, a classifier is a Neural Network which takes as input all physics parameters identifying an event, and produces output which indicates whether the event is recognized as signal or background. Figure 7 gives information about the performance of the constructed classifier.

- **Figure 7a**: a ROC curve which gives information about the success of the classifier. The ROC curve is created by plotting the true positive rate (known as the probability of detection) against the false positive rate (known as the probability of false alarm) at various threshold settings. For the constructed classifier, the area under the ROC curve has a value close to one which indicates great success.
- **Figure 7b**: a histogram of the classifier output for the combination of signal and background simulation in two different regions in $\Delta\varphi$ - $0 < \Delta\varphi \leq 1$ in black and $1 < \Delta\varphi \leq \pi$ in red . Most events are concentrated near the origin, which means that the classifier identifies the majority of the events to be background. This is expected, since the statistics of the signal events are much lower than background.
- **Figure 7c**: a histogram of the classifier output for background events only in two different regions in $\Delta\varphi$.

The constructed classifier is found to have great performance. However, as shown in Figure 7b and Figure 7c, $\Delta\varphi$ is correlated to the classifier output.

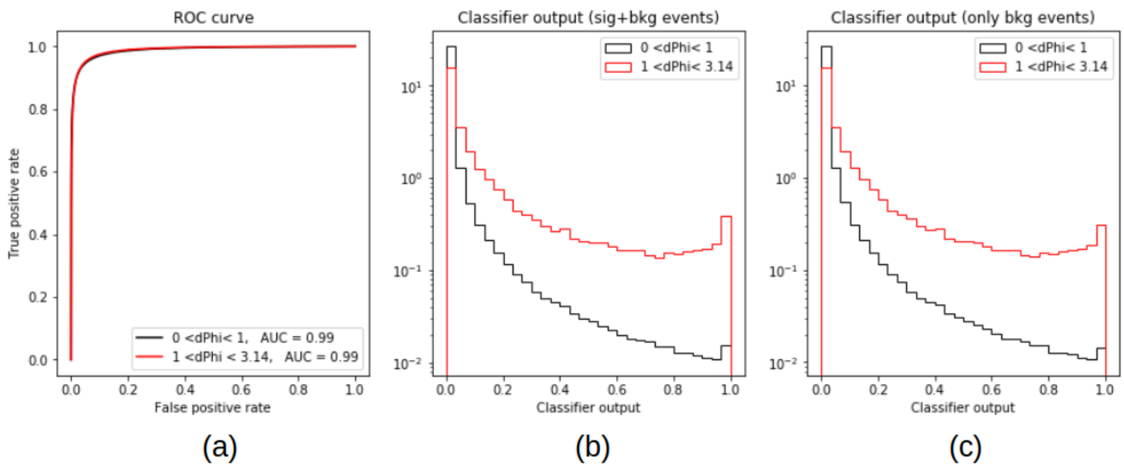

Figure 7: The performance of the classifier. (a) A ROC curve showing successful classification. (b) A histogram of the classifier output for the both signal and background events in two different regions in $\Delta\varphi$. (c) A histogram of the classifier output for background events only in two different regions in $\Delta\varphi$.

4.2 Results for the Adversarial Network

After training the Adversarial Network for different values of λ, it was found that $\lambda = 0.85$ results best decorrelation of classifier output from $\Delta\varphi$ and good performance (see Figure 8).

- **Figure 8a**: an area under the ROC curve indicate successful classification. However, a small kink now appears in the distribution for $1 < \Delta\varphi \leq \pi$ which corresponds to the slight confusion happening to the classifier due to the activity of the adversary.
- **Figure 8b**: most events are still concentrated near the origin, which means that the classifier identifies the majority of events to be background (as expected). The two distributions referring to the two different regions of $\Delta\varphi$ are now much closer in comparison to Figure 7b, which implies that the adversary was successful in the decorrelation of the classifier output from $\Delta\varphi$.
- **Figure 8c**: a histogram similar to Figure 7b but taking into account only background events. Also the two distributions referring to the two different regions of $\Delta\varphi$ are now much closer in comparison to Figure 7c, which implies successful decorrelation.

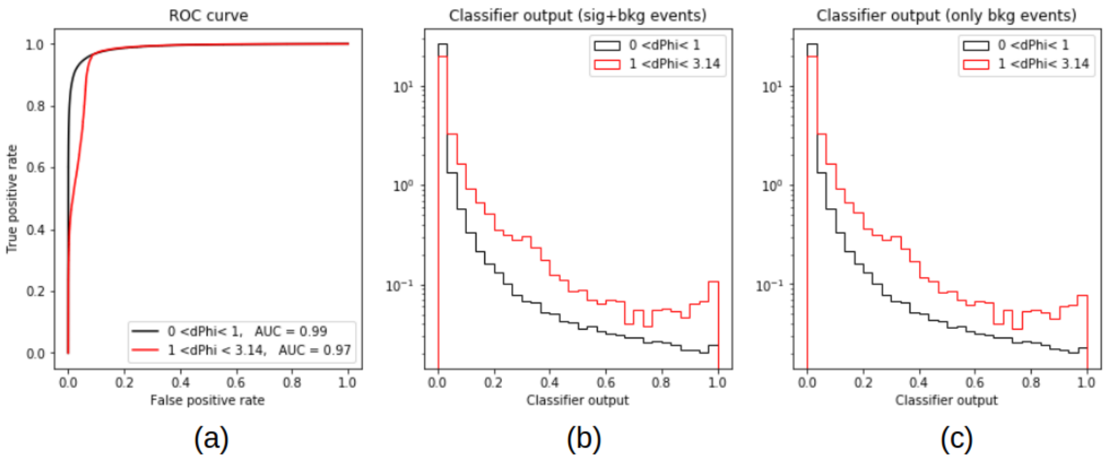

Figure 8: The performance of the Adversarial Network. (a) A ROC curve is represented, showing successful classification, with a kink indicating the confusion due to the adversary. (b) A histogram of the classifier output for the combination of signal and background simulation in two different regions in $\Delta\varphi$. The two distributions are closer in comparison to Figure 7b, which implies successful decorrelation of the classifier output from $\Delta\varphi$. (c) A histogram of the classifier output in two different regions in $\Delta\varphi$ for background events only.

4.3 Comparison

As already mentioned in the previous subsections, from Figure 7b and Figure 8b, it is clear how the two colored distributions for the different range of values of $\Delta\varphi$ become more superimposed for the Adversarial Network, indicating the decorrelation. However, this happens at the expense of classification efficiency which can be seen from the ROC curves in Figure 7a and Figure 8a.

Another point for comparison can be seen from Figure 9. Comparing the resulting Ratio from the two Density plots for each of the two networks, it is found that: $\frac{N_A/N_B}{N_D/N_C} = 0.079$ for the normal classifier, and $\frac{N_A/N_B}{N_D/N_C} = 0.887$ for the Adversarial Network. Note how the resulting Ratio from the Adversarial Network is closer to the value one by an order of magnitude than the resulting Ratio from the normal classifier, possibly allowing for using Data-Driven Background Estimation.

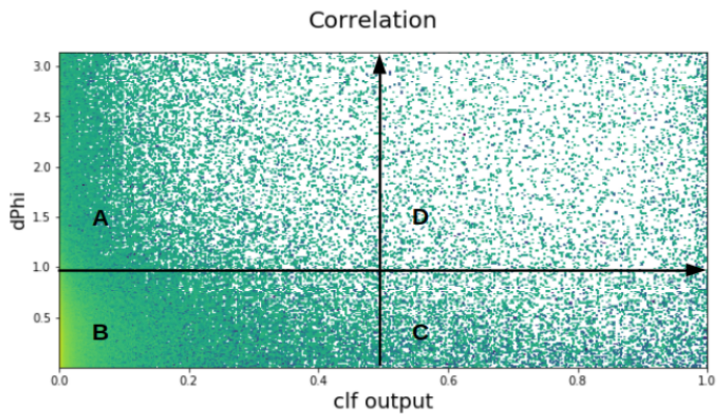

(a)

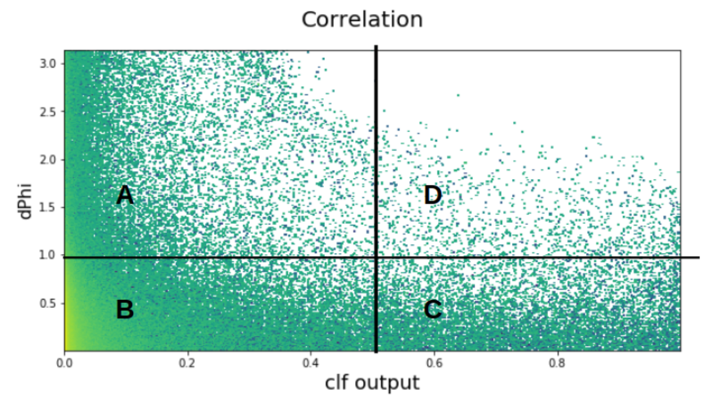

(b)

Figure 9: (a) Density plots for events resulting from the normal classifier. (b) Density plots for events resulting from the Adversarial Network.

4.4 The stability of the Adversarial Network

The stability of the Adversarial Network needs further investigation. For the same network architecture, each training may provide a different result. Figure 10 presents a histogram of 28 different training simulations of the Adversarial Network for the same value of λ. It can be seen that, on average, most simulations give a Ratio close to 0.6-0.8. This small fluctuation is (more or less) expected since the batch selection during the training is chosen randomly. However, few simulations give Ratio values much further from 1.

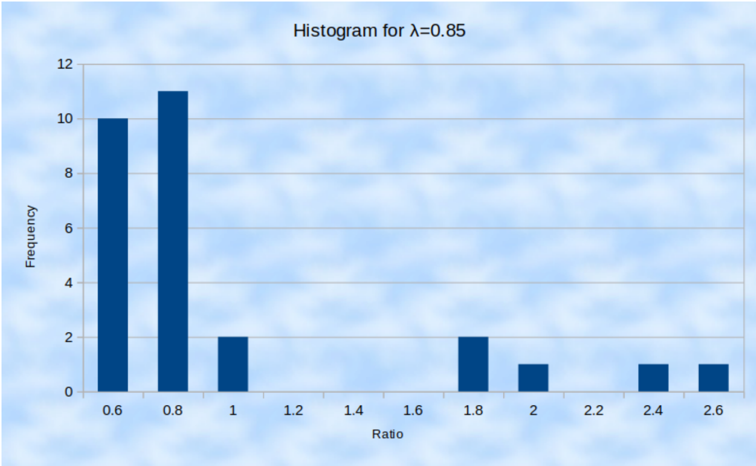

Figure 10: A representation of the Ratio ($\frac{N_A/N_B}{N_D/N_C}$) for 28 training simulations of the Adversarial Network for $\lambda = 0.85$.

5 Conclusion

An Adversarial Network for decorrelating the classifier output from $\Delta\varphi$ at the expense of small classification efficiency loss was developed and studied on Monte Carlo simulated data based on the CMS 2016 experiment [1]. The normal classifier is found to be a more successful signal-to-background classifier than the Adversarial Network. The Adversarial Network can have similar successful performance with the addition of decorrelating the output of the classifier from $\Delta\varphi$.

In future, these studies may be further improved by:

- Conducting further studies of the stability of Adversarial Training.
- Optimizing the hyper-parameter space of both the classifier and the adversary.
- Using the Adversarial Network on data to predict the background in the signal region.

References

[1] CMS collaboration (2017). Search for supersymmetry in events with one lepton and multiple jets in proton-proton collisions at sqrt(s) = 13 TeV. Available at: https://arxiv.org/abs/1609.09386

[2] Goodfellow, I., Pouget-Abadie, J., Mirza, M., Xu, B., Warde-Farley, D., Ozair, S., Courville, A., and Bengio, Y. (2014). Generative adversarial nets. https://arxiv.org/abs/1406.2661

[3] Louppe, G., Kagan, M., and Cranmer, K. (2016). Learning to Pivot with Adversarial Networks. https://arxiv.org/abs/1611.01046

[4] Sander, C. (2012) 'Data Driven Background Estimation [PowerPoint presentation]. Available at: http://www.desy.de/~csander/Talks/120223_SFB_DataDrivenBackgrounds.pdf (Accessed: 24 August 2019).